DYNAMIC FRACTURE AND CRACK ARREST BEHAVIOUR OF A PIPELINE STEEL INVESTIGATED WITH A NEW SPECIMEN GEOMETRY : THE RING TEST

T. IUNG*, M. DI FANT** and A. PINEAU*

A new test specimen geometry was deviced to investigate unstable crack propagation and crack arrest, as well as stable crack growth. This geometry is a cracked ring which is subjected to a compressive load applied at its poles while the crack is located in the equatorial plane at the outer surface of the specimen. One of the main interests of this geometry is the variation of the K factor with crack length which follows a bell-shaped curve. This allows to control the crack velocity by adjusting the initial crack length. The behaviour of a pipeline steel was investigated at 77 K using this test specimen.

INTRODUCTION

Safety consideration for pipelines or nuclear pressure vessels has led to the study of dynamic crack propagation and crack arrest. The standard A.S.T.M. procedure (1) recommends a static analysis of wedge-loaded Compact Crack Arrest (C.C.A.) specimens. But some authors have shown that dynamic effects (2,3) (kinetic energy, wave reflection, inertia...) as well as experimental details (4) (control of the pin loading system and specimen preparation which requires a spot-welded notch) have to be taken into account in the analysis of the test results.

In this paper, we describe an original experiment of dynamic crack propagation and crack arrest. The geometry, a cracked ring, was already tested in thermal shock experiments (4, 5). In the present study, our tests are isothermal and carried out at liquid nitrogen temperature. As recommended by the A.S.T.M., a static approach has been used to analyse the ring test and then to determine the K_{Ia} value of a pipeline mild steel. Quantitative observations of the microdamage in the wake of propagating cracks were made.

* Centre des Matériaux, Ecole des Mines, BP 87 - 91003 EVRY Cedex, URA CNRS n° 866 - France

** IRSID, 34 rue de la Croix de Fer, 78105 St Germain-en-Laye, France.

PRESENTATION OF THE EXPERIMENT

Figure 1 illustrates the principle of the test. The geometry of the ring is defined by the external and internal diameters. A compressive load is applied to the poles of the specimen. An external radial crack is induced by fatigue loading at the equator of the ring. Two dimensionless parameters characterize the geometry : β and λ (see figure 1).

The interest of that geometry lies in the bell-shaped variation of the stress intensity factor, K, with the crack length. The curve (figure 2) was obtained by 2D FEM calculations performed using the ZEBULON code developed in Centre des Matériaux, Ecole des Mines (6). A crack moving along the equator towards the center of the ring will undergo an increasing stress intensity factor, leading to unstable crack propagation, and then a decreasing one, which makes sure of crack arrest. It is worth noting that the decreasing part of the K-λ curve enables us also to study stable crack propagation with long initial cracks.

In the present paper, we are interested in dynamic crack propagation and crack arrest. The event lasts about 30 μs. During this short time, it is reasonable to suppose that the displacement imposed at the poles is constant. It was shown (6) that the hypothesis of constant load gives only a slight difference of about 2 or 3 % with the previous hypothesis.

Twenty-one tests were performed. All rings have an external radius of 65 mm, β being equal to 1/2, and a thickness of 15 mm. The material investigated is a mild steel subjected to a controlled rolling. The ferritic-perlitic microstructure is fine, the grain size is 6 μm. This very clean steel is low alloyed with niobium and vanadium (C = 0,045 % ; Mn = 1,2 % ; Si = 0,25 % ; Nb = 0,04 % ; V = 0,06 % ; S = 0,001 % ; P = 0,007 %). The tests were carried out at 77 K to obtain a brittle behaviour. This results in pure cleavage fracture. The rings were machined in such a way that the crack always propagates along the rolling direction. The crack velocity was measured with a gage glued on the surface of the specimen in the region crossed by the moving crack. This special gage is made of twenty conductive wires connected to a high speed memory oscilloscope.

MECHANICAL RESULTS

It was first checked that the K values at crack initiation were consistent with the fracture toughness of the steel measured from conventional tests carried out on C.T. type specimens, $K_{Ic} = 35\ MPa\sqrt{m}$, which validates our numerical calculations.

Crack speed

Figure 3 shows the typical variation of the measured speed with the crack tip position. During the major part of the jump, the crack runs at constant speed and then slows down until arrest. When the jump was big enough so that the speed

could be measured, the maximum crack speed was found to be between 250 and 920 m/s. The highest speeds were obtained with the shortest cracks, as expected, since in this case, the energy available for crack propagation is more important.

Crack arrest fracture toughness, K_{Ia}

The fracture surfaces were heat tinted (300°C for 1 h) before opening the specimen. The arrest front is then easy to differentiate. The length at arrest is determined as recommended in K_{Ic} A.S.T.M. standards (7).

Knowing this value, the stress intensity factor at arrest deduced from figure 2 gives the crack arrest fracture toughness of the steel by adopting a static approach. All the results are reported in figure 4. These results show a large scatter which is discussed in the following. It is observed that if the maximum crack speed is lower than 400 or 500 m/s, K_{Ia} is of the same order as K_{Ic}. Beyond 500 m/s, K_{Ia} decreases strongly to reach values which are very close to zero. It is worth noting that these low values were obtained for the smallest cracks which arrested at crack length corresponding to the steepest gradient of the K–λ curve.

METALLURGICAL OBSERVATIONS

Macroscopic unbroken ligaments were observed on the fracture surface of a number of specimens. This observation has already been reported by other authors (e.g. 3). It is felt that this is one of the explanation of the scatter in K_{Ia} value. Indeed, two specimens exhibited a maximum crack speed of 650 m/s giving two widely different values of K_{Ia}. A lot of unbroken ligaments were found on the first one's fracture surface (K_{Ia} = 35 MPa$\sqrt{m}$) whereas none could be seen on the second one's (K_{Ia} = 5 MPa$\sqrt{m}$). These ligaments give rise to a crack tip shielding effect. The origin of this phenomenon is not yet fully understood.

Microscopic damage located just below the fracture surface was also examined on tranverse sections by optical and scanning electron microscopy. Cleavage microcracks were observed along the crack path (figure 5). After polishing and slight etching, the linear density was measured (figure 6). The cracks are all the more numerous as the crack speed is high, their size being constant.

Mechanical twinning was also observed under the fracture surface as shown in figure 5 where it is noticed that one cleavage microcrack was nucleated at the intersection of two twins. It is well known that mechanical twinning is initiated at very low temperatures and very high strain rates. High strain rate compression tests ($\dot{\varepsilon}$ = 1200 s^{-1}) were carried out on our material at 77 K by using Hopkinson bars but no twins could be observed after deformation. This suggests that the strain rate at the tip of a moving crack might be significantly larger than $10^3 s^{-1}$.

CONCLUSION

1. The ring test presented in this study proved to be a very convenient way to study dynamic crack propagation and crack arrest. The crack velocity can be controlled by adjusting the initial crack length. In this study, maximum crack speeds of 920 m/s were reached.

2. The values of crack arrest fracture toughness, K_{Ia}, as inferred from a static approach show, in spite of a large scatter, a clear tendancy to decrease when the crack velocity is increased. Extremely low values of K_{Ia} are obtained when the crack speed exceeds 500 m/s.

3. The microdamage in the plastic wake of the propagating crack characterized by the presence of secondary cleavage microcracks is related to the crack velocity. In particular, the number of microcracks is an increasing function of crack speed.

4. Mechanical twinning was observed in the plastic wake of propagating cracks. This suggests that the strain rate ahead of a propagating crack might be larger than $1200\ s^{-1}$.

ACKNOWLEDGEMENTS

Financial support from Institut de Recherche de la Sidérurgie française and from Ministère de la Recherche et de la Technologie is greatly acknowledged.

REFERENCES

(1) "Standard Test Method for Determining Plane – Strain Crack Arrest Fracture Toughness, K_{Ia}, of Ferritic Steels", ASTM–E 1221, 1988.

(2) Hahn G.T., Hoagland R.G., Rosenfield A.R., Kanninen M.F., "A Preliminary Study of Fast Fracture and Arrest in D.C.B. Test Specimens", Proceeding of an International Conference on "Dynamic Crack Propagation", Edited by G. Sih, Nordhoff International Publishing, England, 1972.

(3) Kalthoff J.F., "Experimental Fracture Dynamics" in "Crack Dynamics in Metallic Materials", Edited by J.R. Klepaczko, Springer Verlag, 1990.

(4) Di Fant M., Fontaine A., Pineau A., "Dynamic Crack Propagation and Crack Arrest in a Structural Steel : Comparison Between Isothermal and Thermal Shock Tests" in "Dynamic Failure of Materials. Theory Experiments and Numerics", Edited by Rossmanith H.P. and Rosakis A.J., Elsevier Applied Science, 1991.

(5) Cheverton R.D., Gehlen P.E., Hahn G.T., Iokander S.K., "Application of Crack Arrest Theory to a Thermal Shock Experiment" in "Crack Arrest Methodology and Applications", ASTM–STP 711, Edited by Hahn G.T. and Kanninen M.F., England, 1980.

(6) Iung T., Pineau A., "Résistance à la Rupture Dynamique d'Aciers pour Gazoducs", IRSID, France, Internal Report 92.303, 1992.

(7) "Standard Test Method for Plane–Strain Fracture Toughness of Metallic Materials", ASTM – E 399, 1984.

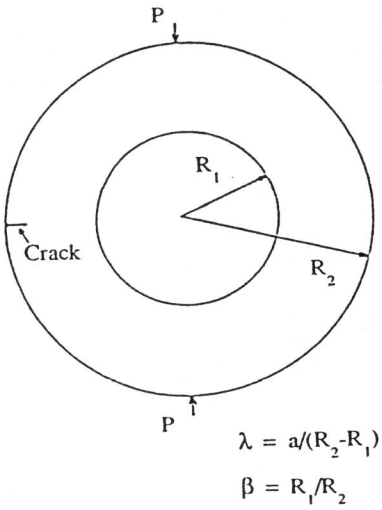

Figure 1 : Geometry of the ring specimen.

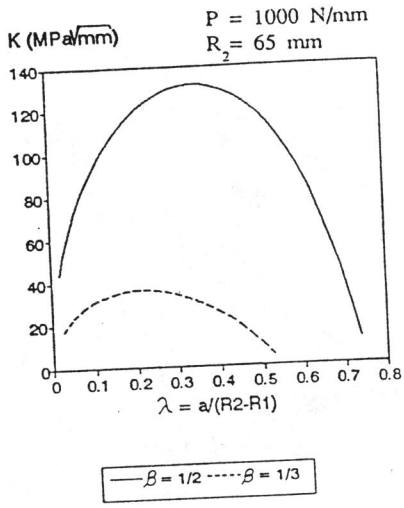

Figure 2 : K–λ curves for different β.

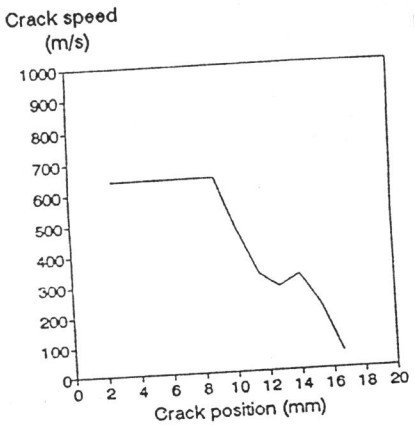

Figure 3 : Variation of the crack speed during the jump.

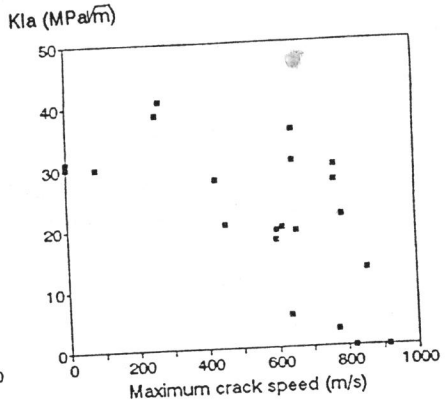

Figure 4 : Variation of K_{Ia} with maximum crack speed.

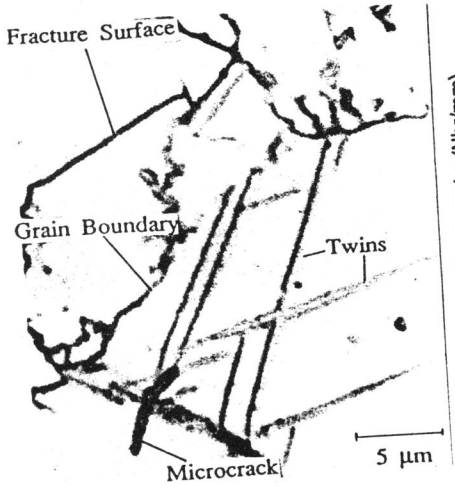

Figure 5 : Optical micrograph of microcrack and twins.

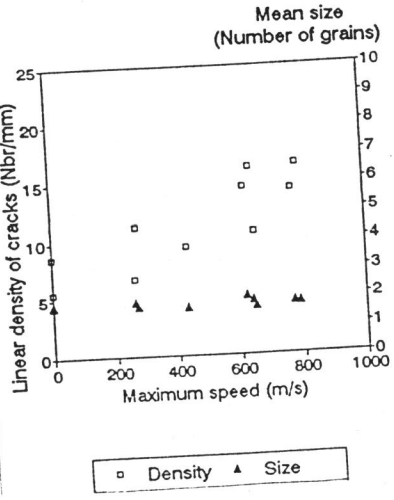

Figure 6 : Linear density and mean size of the microcracks.